Article

On [FeS]–(□-SR)–M Bridge Formation in the Synthesis of an A-Cluster Analogue of Carbon Monoxide Dehydrogenase/Acetylcoenzyme A Synthase

P. Venkateswara Rao, Sumit Bhaduri, Jianfeng Jiang, Daewon Hong, and R. H. Holm

J. Am. Chem. Soc., **2005**, 127 (6), 1933-1945• DOI: 10.1021/ja040222n • Publication Date (Web): 20 January 2005

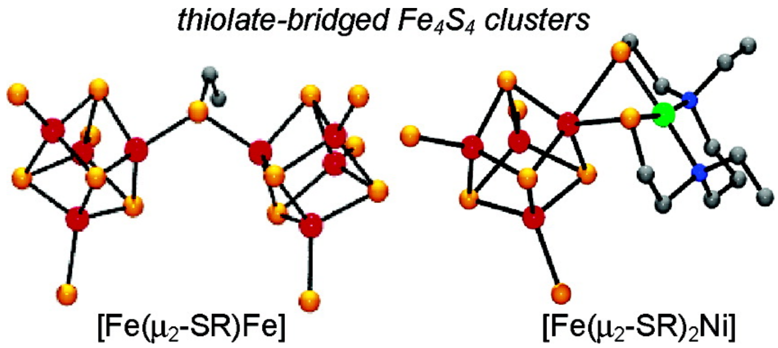

Journal of the American Chemical Society is published by the American Chemical Society. 1155 Sixteenth Street N.W., Washington, DC 20036

J|A|C|S
ARTICLES

On $[Fe_4S_4]^{2+}-(\mu_2\text{-}SR)-M^{II}$ Bridge Formation in the Synthesis of an A-Cluster Analogue of Carbon Monoxide Dehydrogenase/Acetylcoenzyme A Synthase

P. Venkateswara Rao, Sumit Bhaduri, Jianfeng Jiang, Daewon Hong, and
R. H. Holm*

Contribution from the Department of Chemistry and Chemical Biology, Harvard University, Cambridge, Massachusetts 02138

Received September 22, 2004; E-mail: holm@chemistry.harvard.edu

Abstract: The construction of a synthetic analogue of the A-cluster of carbon monoxide dehydrogenase/acetylcoenzyme synthase, the site of acetylcoenzyme A formation, requires as a final step the formation of an unsupported $[Fe_4S_4]-(\mu_2\text{-}SR)-Ni^{II}$ bridge to a preformed cluster. Our previous results (Rao, P. V.; Bhaduri, S.; Jiang, J.; Holm, R. H. *Inorg. Chem.* **2004**, *43*, 5833) and the work of others have addressed synthesis of dinuclear complexes relevant to the A-cluster. This investigation concentrates on reactions pertinent to bridge formation by examining systems containing dinuclear and mononuclear Ni^{II} complexes and the 3:1 site-differentiated clusters $[Fe_4S_4(LS_3)L']^{2-}$ ($L' = TfO^-$ (**14**), SEt (**15**)). The system **14**/$[\{Ni(L_O\text{-}S_2N_2)\}M(SCH_2CH_2PPh_2)]^+$ results in cleavage of the dinuclear complex and formation of $[\{Ni(L_O\text{-}S_2N_2)\}\text{-}Fe_4S_4(LS_3)]^-$ (**18**), in which the Ni^{II} complex binds at the unique cluster site with formation of a $Ni(\mu_2\text{-}SR)_2Fe$ bridge rhomb. Cluster **18** and the related species $[\{Ni(phma)\}Fe_4S_4(LS_3)]^{3-}$ (**19**) are obtainable by direct reaction of the corresponding cis-planar $Ni^{II}-S_2N_2$ complexes with **14**. The mononuclear complexes $[M(pdmt)(SEt)]^-$ ($M = Ni^{II}$, Pd^{II}) with **14** in acetonitrile or Me_2SO solution react by thiolate transfer to give **15** and $[M_2(pdmt)_2]$. However, in dichloromethane the Ni^{II} reaction product is interpreted as $[\{Ni(pdmt)(\mu_2\text{-}SEt)\}Fe_4S_4(LS_3)]^{2-}$ (**20**). Reaction of Et_3NH^+ and **15** affords the double cubane $[\{Fe_4S_4(LS_3)\}_2(\mu_2\text{-}SEt)]^{3-}$ (**21**). Cluster **18** contains two mutually supportive $Fe-(\mu_2\text{-}SR)-Ni^{II}$ bridges, **19** exhibits one strong and one weaker bridge, **20** has one unsupported bridge (inferred from the ^1H NMR spectrum), and **21** has one unsupported $Fe-(\mu_2\text{-}SR)-Fe$ bridge. Bridges in **18**, **19**, and **21** were established by X-ray structures. This work demonstrates that a bridge of the type found in the enzyme A-clusters is achievable by synthesis and implies that more stable, unsupported single thiolate bridges may require reinforcement by an additional covalent linkage between the Fe_4S_4 and nickel-containing components. (LS_3 = 1,3,5-tris((4,6-dimethyl-3-mercaptophenyl)thio)-2,4,6-tris(*p*-tolylthio)benzene(3−); $L_O\text{-}S_2N_2$ = *N*,*N*′-diethyl-3,7-diazanonane-1,9-dithiolate(2−); pdmt = pyridine-2,6-methanedithiolate(2−); phma = *N*,*N*′-1,2-phenylenebis(2-acetylthio)-acetamidate(4−); TfO = triflate.)

Introduction

Bifunctional carbon monoxide dehydrogenases (CODH/ACS) contain two catalytic centers composed of Ni−Fe−S clusters.[1−3] The reaction $CO + H_2O \rightleftharpoons CO_2 + 2H^+ + 2e^-$ is catalyzed at the C-cluster. X-ray structures of enzymes from two different organisms reveal a $NiFe_3S_{4,5}$ core with a $NiFe_3S_4$ cuboidal portion to which is attached an exo-iron atom.[4−6] At the A-cluster, acetylcoenzyme A is synthesized from coenzyme A, a methyl group derived from a corrinoid protein, and carbon monoxide. The site, shown in Figure 1, has the minimal formulation $[Fe_4S_4]-(\mu_2\text{-}S_{Cys})-[Ni((\mu_2\text{-}S_{Cys})_2Gly)Ni]$. From crystallographic and X-ray absorption spectroscopic results on enzymes from *Moorella thermoacetica* and *Carboxydothermus hydrogenoformans*, the Ni^{II} atom distal to the cluster is coordinated in a cis-planar $Ni^{II}-S_2N_2$ arrangement. The proximal Ni^{II} atom is part of a $Ni_2(\mu_2\text{-}SR)_2$ bridge rhomb and is implicated in a tetrahedral $Ni^{II}(\mu_2\text{-}S_{Cys})_3L$ coordination unit with

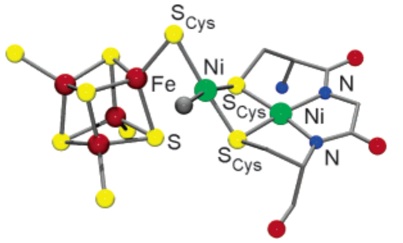

Figure 1. Structure of the bridged assembly $[Fe_4S_4]-(\mu_2\text{-}S_{Cys})-Ni_p-(\mu_2\text{-}S_{Cys})_2-Ni_d$, which is the A-cluster of *Moorella thermoacetica* (d = distal, p = proximal to the cluster). The distal Ni^{II} atom is bound by a deprotonated Cys-Gly-Cys sequence; one ligand at the Ni_p site is unidentified.

---

(1) Ragsdale, S. W.; Kumar, M. *Chem. Rev.* **1996**, *96*, 2515−2539.
(2) Grahame, D. A. *Trends Biochem. Sci.* **2003**, *28*, 221−224.
(3) Drennan, C. L.; Peters, J. W. *Curr. Opin. Struct. Biol.* **2003**, *13*, 220−226.
(4) Drennan, C. L.; Heo, J.; Sintchak, M. D.; Schreiter, E.; Ludden, P. W. *Proc. Natl. Acad. Sci. U.S.A.* **2001**, *98*, 11973−11978.
(5) Dobbek, H.; Svetlitchnyi, V.; Gremer, L.; Huber, R.; Meyer, O. *Science* **2001**, *293*, 1281−1285.
(6) Dobbek, H.; Svetlitchnyi, V.; Liss, J.; Meyer, O. *J. Am. Chem. Soc.* **2004**, *126*, 5382−5387.

10.1021/ja040222n CCC: $30.25 © 2005 American Chemical Society

an unidentified ligand.[7−9] This structure also appears to apply to acetyl-CoA decarbonylase/synthase from *Methanosarcina thermophilia*.[10] In addition, structures have been reported in which Cu(I)[11,12] and Zn(II)[8] atoms occupy the proximal site. However, current evidence is persuasive in establishing Ni^{II} as the native metal in this site.[8,13−15]

We are engaged in the problem of constructing analogues of both the C-cluster and A-cluster of CODH/ACS, a prerequisite to subsequent structural and reactivity studies. Recent progress on the C-cluster problem is described elsewhere.[16] Here we proceed on the basis of an Fe_4S_4−Ni−Ni A-cluster. As set out earlier,[17] synthesis of an A-cluster analogue involves three steps: (i) preparation of a cis-planar Ni_d^{II}-S_2N_2 unit with physiologically realistic coordination; (ii) introduction of a Ni_p^{II} bridging atom to afford a doubly bridged $Ni_2(\mu_2\text{-SR})_2$ rhomb; and (iii) formation of a $[Fe_4S_4]-(\mu_2\text{-SR})-Ni_p^{II}$ bridge to a preformed cubane-type cluster with the desired stereochemistry at the proximal site. Step (i) has been addressed in two independent studies. Krishnan and Riordan[18] have prepared a dianionic $Ni^{II}-S_2N_2$ complex ligated by a substituted Cys-Gly-Cys peptide. In our work, we have synthesized and structurally characterized a mononuclear Ni^{II} complex derived from a tetradeprotonated diamidodithiolate ligand.[17] Both complexes have the 6−5−5 chelate ring size pattern of the A-cluster. The mean bond lengths Ni−S (2.17 Å) and Ni−N (1.88 Å) in $[Ni(L\text{-}655)]^{2-}$ agree well with values at the Ni_d^{II} protein site.[7,9] Step (ii) has been pursued by the preparation of several *dinuclear* complexes which contain nonplanar $Ni^{II}_2(\mu_2\text{-SR})_2$ rhombs.[17−19] For example, in this laboratory we have prepared and structurally defined the complexes $[\{Ni(L\text{-}655)\}Ni(R_2PCH_2CH_2PR_2)]$ (R = Et, Ph), in which phosphine-bound Ni^{II} occupies what would be the proximal site in a fully developed analogue assembly. We have also structurally defined bridging modes between several other cis-planar $Ni^{II}-S_2N_2$ complexes and Ni^{II}, $Cu^{I,II}$, Zn^{II}, and Hg^{II}. When these results and those of others are compiled, over 20 different bridging modalites involving one or both thiolate sulfur atoms emerge.[17] One of these, $Ni^{II}_2(\mu_2\text{-SR})_2$, has been integrated into the native catalytic site.

Step (iii) appears to be most precarious in the construction of an analogue site cluster. Thus far, the minimal construct $[Fe_4S_4]^{2+}-(\mu_2\text{-SR})-M$, where M is a mononuclear entity, has not been directly demonstrated by an X-ray structure determination. In one instance, formation of this entity with M = Fe^{II} was indicated by ^1H NMR shifts, but the lability of the bridge precluded specific recognition and isolation of the desired species.[20] Using a de novo designed helix−loop−helix peptide as a scaffold, the unit $[Fe_4S_4]^{2+}-(\mu_2\text{-}S_{Cys})-Ni^{II}(S_{Cys})(N_{His})_2$ was constructed in a process in which the Ni^{II} component was added to the peptide containing the cluster.[21] Bridge formation is supported by EXAFS results.[22] Sulfido-bridged units $[Fe_4S_4]^{2+}-(\mu_2\text{-S})-Fe^{III}$ have been isolated and identified by ^1H NMR isotropic shifts.[23,24] The only crystallographically proven instances of thiolate bridging to an Fe_4S_4 cluster in stable species are found with $[\{Ni^{II}(L_O\text{-}S_2N_2)\}Fe_4S_4I_3]^-$ [25] and $[\{Ni^{II}(L_O\text{-}S_2N_2)\}_2Fe_4S_4L_2]$ (L = I^-, RS^-),[26] where the Ni^{II} complex functions as a bidentate ligand in the development of five-coordinate iron sites. Here we describe our observations pursuant to step (iii), the formation of bridged clusters relevant to the A-cluster structure.

Experimental Section

Preparation of Compounds. All operations were conducted under a pure dinitrogen atmosphere box. Numerical designations of complexes and abbreviations are given in Chart 1. All solvents were distilled prior to use, as described elsewhere.[17] Selected compounds were identified by electrospray mass spectrometry (percentages refer to peak intensities relative to the most intense fragment peak). Certain compounds were analyzed; 12 compounds were characterized by X-ray structure determinations.

$[Pt(SCH_2CH_2PPh_2)(PPh_3)Cl]$ (1). To a solution of $[PtCl_2(PPh_3)_2]$ (0.451 g, 0.57 mmol) in 30 mL of dichloromethane was added slowly a solution of $HSCH_2CH_2PPh_2$[27] (0.148 g, 0.60 mmol) in 5 mL of dichloromethane. The color of the solution turned from yellow to yellow-orange. The mixture was stirred for 3 h, and the volume was reduced to 5 mL. Hexanes (20 mL) were added, and the solution was allowed to stand at −20 °C overnight. The product was filtered off, washed with hexanes, and dried; it was obtained as 0.330 g (78%) of yellow microcrystals. Mass spectrum: *m/z* 702.0 ($\{M - Cl^-\}^+$, 100%). Anal. Calcd for $C_{32}H_{29}ClP_2PtS$: C, 52.07; H, 3.96; S, 4.34. Found: C, 52.25; H, 4.06; S, 4.46.

$(Bu_4N)[Pd(pdmt)(SEt)]$ ($(Bu_4N)[2]$). To an orange suspension of $[Pd(pdmt)]_2$[28] (0.110 g, 0.20 mmol) in 30 mL of acetonitrile were added NaSEt (0.034 g, 0.40 mmol) and Bu_4NBr (0.129 g, 0.40 mmol). Upon stirring, the orange-yellow slurry turned to a transparent orange-red solution in 3 h, after which the solution was filtered through Celite and the solvent removed in vacuo. The orange oil was triturated with ether to afford an orange-red solid. Recrystallization of the solid from acetonitrile/ether afforded the product as 0.135 g (54%) of orange crystals. ^1H NMR (CD_3CN, anion): δ 1.18 (t, 3), 2.20 (q, 2), 4.20 (s, 4), 7.14 (d, 2), 7.40 (t, 1). Mass spectrum: *m/z* 332 (M^-, 100%). Anal. Calcd for $C_{25}H_{48}N_2PdS_3$: C, 51.83; H, 8.35; N, 4.84; S, 16.61. Found: C, 51.68; H, 8.31; N, 4.73; S, 16.55.

$[\{Ni(L_O\text{-}S_2N_2)\}FeCl_2]$ (4). To a solution of $[Ni(L_O\text{-}S_2N_2)]$[26] (0.062 g, 0.20 mmol) in 5 mL of acetonitrile was added a pale suspension of $FeCl_2$ (0.026 g, 0.20 mmol) in 2 mL of acetonitrile. The mixture was stirred for 2 h. The dark red solution was filtered through Celite, and

---

(7) Russell, W. K.; Stålhandske, C. M. V.; Xia, J.; Scott, R. A.; Lindahl, P. A. *J. Am. Chem. Soc.* **1998**, *120*, 7502−7510.

(8) Darnault, C.; Volbeda, A.; Kim, E. J.; Legrand, P.; Vernède, X.; Lindahl, P. A.; Fontecilla-Camps, J. C. *Nature Struct. Biol.* **2003**, *10*, 271−279.

(9) Svetlitchnyi, V.; Dobbek, H.; Meyer-Klaucke, W.; Meins, T.; Thiele, B.; Römer, P.; Huber, R.; Meyer, O. *Proc. Natl. Acad. Sci. U.S.A.* **2004**, *101*, 446−451.

(10) Funk, T.; Gu, W.; Friedrich, S.; Wang, H.; Gencic, S.; Grahame, D. A.; Cramer, S. P. *J. Am. Chem. Soc.* **2004**, *126*, 88−95.

(11) Doukov, T. I.; Iverson, T. M.; Seravalli, J.; Ragsdale, S. W.; Drennan, C. L. *Science* **2002**, *298*, 567−572.

(12) Seravalli, J.; Gu, W.; Tam, A.; Strauss, E.; Begley, T. P.; Cramer, S. P.; Ragsdale, S. W. *Proc. Natl. Acad. Sci. U.S.A.* **2003**, *100*, 3689−3694.

(13) Bramlett, M. R.; Tan, X.; Lindahl, P. A. *J. Am. Chem. Soc.* **2003**, *125*, 9316−9317.

(14) Schenker, R. P.; Brunold, T. C. *J. Am. Chem. Soc.* **2003**, *125*, 13962−13963.

(15) Seravalli, J.; Xiao, Y.; Gu, W.; Cramer, S. P.; Antholine, W. E.; Krymov, V.; Gerfern, G. J.; Ragsdale, S. W. *Biochemistry* **2004**, *43*, 3944−3955.

(16) Panda, R.; Zhang, Y.; McLauchlan, C. C.; Venkateswara Rao, P.; Tiago de Oliveira, F. A.; Münck, E.; Holm, R. H. *J. Am. Chem. Soc.* **2004**, *126*, 6448−6459.

(17) Rao, P. V.; Bhaduri, S.; Jiang, J.; Holm, R. H. *Inorg. Chem.* **2004**, *43*, 5833−5849.

(18) Krishnan, R.; Riordan, C. G. *J. Am. Chem. Soc.* **2004**, *126*, 4484−4485.

(19) Wang, Q.; Blake, A. J.; Davies, E. S.; McInnes, E. J. L.; Wilson, C.; Schröder, M. *Chem. Commun.* **2003**, 3012−3013.

(20) Liu, H. Y.; Scharbert, B.; Holm, R. H. *J. Am. Chem. Soc.* **1991**, *113*, 9529−9539.

(21) Laplaza, C. E.; Holm, R. H. *J. Am. Chem. Soc.* **2001**, *123*, 10255−10264.

(22) Musgrave, K. B.; Laplaza, C. E.; Holm, R. H.; Hedman, B.; Hodgson, K. O. *J. Am. Chem. Soc.* **2002**, *124*, 3083−3092.

(23) Cai, L.; Holm, R. H. *J. Am. Chem. Soc.* **1994**, *116*, 7177−7188.

(24) Zhou, C.; Cai, L.; Holm, R. H. *Inorg. Chem.* **1996**, *35*, 2767−2772.

(25) Osterloh, F.; Saak, W.; Haase, D.; Pohl, S. *Chem. Commun.* **1996**, 777−778.

(26) Osterloh, F.; Saak, W.; Pohl, S. *J. Am. Chem. Soc.* **1997**, *119*, 5648−5656.

(27) Chatt, J.; Dilworth, J. R.; Schmutz, J. A. *J. Chem. Soc., Dalton Trans.* **1979**, 1595−1599.

(28) Márquez, V. E.; Anacona, J. R. *Polyhedron* **1997**, *16*, 1931−1935.

Chart 1. Designation of Complexes and Abbreviations

$[Pt(SCH_2CH_2PPh_2)(PPh_3)Cl]$	**1**
$[M(pdmt)(SEt)]^{1-}$	M = Ni **2a**,[33] Pd **2b**
$[Ni(L_O\text{-}S_2N_2)]$	**3**[26,34]
$[\{Ni(L_O\text{-}S_2N_2)\}FeCl_2]$	**4**
$[\{Ni(L_O\text{-}S_2N_2)\}_2Ni]^{2+}$	**5**
$[\{Ni(L_O\text{-}S_2N_2)\}Pd(PPh_3)Cl]^{1+}$	**6**
$[\{Ni(L_O\text{-}S_2N_2)\}Pt(PPh_3)Cl]^{1+}$	**7**
$[\{Ni(L_O\text{-}S_2N_2)\}Ni(SCH_2CH_2PPh_2)]^{1+}$	**8**
$[\{Ni(L_O\text{-}S_2N_2)\}Pd(SCH_2CH_2PPh_2)]^{1+}$	**9**
$[\{Ni(L_O\text{-}S_2N_2)\}Pt(SCH_2CH_2PPh_2)]^{1+}$	**10**
$[Ni(L\text{-}655)]^{2-}$	**11**[17]
$[\{Ni(L\text{-}655)\}_2Ni]^{2-}$	**12**[17]
$[\{Ni(L\text{-}655)\}Pt(PPh_3)_2]$	**13**
$[Fe_4S_4(LS_3)(OTf)]^{2-}$	**14**[31]
$[Fe_4S_4(LS_3)(SEt)]^{2-}$	**15**[23]
$[Fe_4S_4(LS_3)Cl]^{2-}$	**16**[35]
$[Fe_4S_4(LS_3)(bdt)]^{3-}$	**17**[36]
$[\{Ni(L_O\text{-}S_2N_2)\}Fe_4S_4(LS_3)]^{1-}$	**18**
$[\{Ni(phma)\}Fe_4S_4(LS_3)]^{3-}$	**19**
$[\{Ni(pdmt)(SEt)\}Fe_4S_4(LS_3)]^{2-}$	**20**
$[\{Fe_4S_4(LS_3)\}_2(SEt)]^{3-}$	**21**

ACS, acetylcoenzyme A synthase; bdt, benzene-1,2-dithiolate(2-); CODH, carbon monoxide dehydrogenase; d, distal; L-655, *N*-(2-mercaptopropyl)-*N'*-(2'-mercaptoethyl)glycinamide(4-); L_O-S_2N_2, *N,N'*-diethyl-3,7-diazanonane-1,9-dithiolate(2-); LS_3, 1,3,5-tris((4,6-dimethyl-3-mercaptophenyl)thio)-2,4,6-tris(*p*-tolylthio)benzene(3-) (3LS = LS_3); OTf, triflate(1-); p, proximal; pdmt, pyridine-2,6-dimethanethiolate(2-); phma, *N,N'*-1,2-phenylenebis(2-acetylthio)acetamidate(4-); Stibt, 2,4,6-triisopropylbenzenethiolate(1-); tdt, toluene-3,4-dithiolate(2-)

ether was diffused into the filtrate. The product was obtained as 0.052 g (62%) of dark red blocklike crystals. Mass spectrum: *m*/*z* 307 ({M − $FeCl_2$ + H^+}$^+$, 100%). Anal. Calcd for $C_{11}H_{24}Cl_2FeN_2NiS_2$: C, 30.45; H, 5.58; N, 6.46; S, 14.78. Found: C, 30.39; H, 5.46; N, 6.40; S, 14.64.

$[\{Ni(L_O\text{-}S_2N_2)\}_2Ni][Ni(PPh_3)Cl_3]_2$ ([5][Ni(PPh$_3$)Cl$_3$]$_2$). To a solution of $[Ni(L_O\text{-}S_2N_2)]$ (0.031 g, 0.10 mmol) in 5 mL of acetonitrile was added a blue-green suspension of $[Ni(PPh_3)_2Cl_2]$ (0.066 g, 0.10 mmol) in 3 mL of acetonitrile. The mixture was stirred for 10 min. The dark brown-green solution was treated with a suspension of $NaPF_6$ (0.017 g, 0.10 mmol) in 1 mL of acetonitrile and stirred for 2 h. The mixture was filtered through Celite, and the filtrate was concentrated to dryness. The dark brown-green solid was dissolved in acetonitrile and filtered, and ether was diffused into the filtrate. The product was obtained as 0.041 g (54%) of brown-green platelike crystals. Mass spectrum: *m*/*z* 336 ({M^{2+}/2}, 100%).

$[\{Ni(L_O\text{-}S_2N_2)\}Pd(PPh_3)Cl](PF_6)$ ([6](PF$_6$)). To a solution of $[Ni(L_O\text{-}S_2N_2)]$ (0.053 g, 0.17 mmol) in 5 mL of acetonitrile was added an orange suspension of *trans*-$[Pd(PPh_3)_2Cl_2]$ (0.119 g, 0.17 mmol) in 5 mL of acetonitrile. The mixture was stirred for 10 min. The dark red solution was treated with a suspension of $NaPF_6$ (0.029 g, 0.17 mmol) in 2 mL of acetonitrile and stirred for 2.5 h. The mixture was filtered through Celite, and the filtrate was evaporated to dryness. The red solid was dissolved in acetonitrile and filtered, and ether was diffused into the filtrate. The product was obtained as 0.107 g (73%) of red platelike crystals. Mass spectrum: *m*/*z* 711 (M^+, 100%). Anal. Calcd for $C_{29}H_{39}ClF_6N_2NiP_2PdS_2$: C, 40.68; H, 4.59; N, 3.37; S, 7.49. Found: C, 40.61; H, 4.63; N, 3.38; S, 7.37.

$[\{Ni(L_O\text{-}S_2N_2)\}Pt(PPh_3)Cl](PF_6)$ ([7](PF$_6$)). The preceding preparation was followed on the same scale with use of *trans*-$[Pt(PPh_3)_2Cl_2]$. The product was obtained as 0.125 g (78%) of red platelike crystals. Mass spectrum: *m*/*z* 799 (M^+, 70%).

$[\{Ni(L_O\text{-}S_2N_2)\}Ni(SCH_2CH_2PPh_2)](PF_6)$ ([8](PF$_6$)). To a suspension of $[Ni(L_O\text{-}S_2N_2)]$ (0.031 g, 0.10 mmol) in 6 mL of THF was added dropwise a dark red solution of $[Ni(SCH_2CH_2PPh_2)Cl]_2$[29] (0.034 g, 0.05 mmol) in 5 mL of THF. The initial suspension slowly disappeared, and a brownish-red solution formed. To the solution was added a suspension of $NaPF_6$ (0.017 g, 0.10 mmol) in 2 mL of THF; the dark red solution was stirred for 3 h. The mixture was filtered through Celite, and the filtrate was concentrated to dryness. A red solid was extracted from the residue with dichloromethane, the extract was filtered, and ether was diffused into the filtrate. The product was obtained as 0.042 g (55%) of red crystals. Mass spectrum: *m*/*z* 611 (M^+, 100%). Anal. Calcd for $C_{25}H_{38}F_6N_2Ni_2P_2S_3$: C, 39.71; H, 5.07; N, 3.79; S, 12.72. Found: C, 39.63; H, 5.15; N, 3.75; S, 12.70.

$[\{Ni(L_O\text{-}S_2N_2)\}Pd(SCH_2CH_2PPh_2)](PF_6)$ ([9](PF$_6$)). To a solution of $[Ni(L_O\text{-}S_2N_2)]$ (0.061 g, 0.20 mmol) in 3 mL of acetonitrile was

---

(29) Gerdau, T.; Klein, W.; Kramolowsky, R. *Cryst. Struct. Commun.* **1982**, *11*, 1663−1669.

added a suspension of $[Pd(SCH_2CH_2PPh_2)(PPh_3)Cl]$[30] (0.130 g, 0.20 mmol) in 3 mL of acetonitrile. To the red solution was added a suspension of $NaPF_6$ (0.034 g, 0.20 mmol) in 3 mL of acetonitrile. The dark red solution was stirred for 3 h and filtered through Celite, and the filtrate was concentrated to 5 mL. Ether was diffused into the filtrate. The product was collected as 0.120 g (75%) of red crystals. Mass spectrum: *m/z* 659 (M^+, 100%). Anal. Calcd for $C_{25}H_{38}F_6N_2Pd_2P_2S_3$: C, 37.35; H, 4.76; N, 3.48; S, 11.97. Found: C, 37.46; H, 4.83; N, 3.50; S, 11.90.

[{Ni(L_O-S_2N_2)}Pt($SCH_2CH_2PPh_2$)](PF_6) ([10](PF_6)). To a solution of $[Ni(L_O\text{-}S_2N_2)]$ (0.061 g, 0.20 mmol) in 5 mL of acetonitrile was added a suspension of $[Pt(SCH_2CH_2PPh_2)(PPh_3)Cl]$ (0.148 g, 0.20 mmol) in 5 mL of acetonitrile. The red solution was treated with a suspension of $NaPF_6$ (0.034 g, 0.20 mmol) in 2 mL of acetonitrile, and the dark red solution was stirred for 3 h. The mixture was filtered through Celite, and ether was diffused into the filtrate. The product was obtained as 0.137 g (77%) of red crystals. Mass spectrum: *m/z* 747 (M^+, 100%).

[{Ni(L-655)}Pt(PPh_3)$_2$] ([13]). *Method A*: To a solution of $(Et_4N)_2[Ni(L\text{-}655)]$[17] (0.040 g, 0.075 mmol) in 3 mL of acetonitrile was added a suspension of $[Pt(SCH_2CH_2PPh_2)(PPh_3)Cl]$ (0.055 g, 0.075 mmol) in 6 mL of acetonitrile; THF (6 mL) was added, and mixture was stirred for 5 h. The mixture was filtered through Celite, and the filtrate was concentrated to dryness. The orange solid was washed twice with acetonitrile and once with ether. An orange solid was extracted from the residue with dichloromethane, the extract was filtered, and ether was diffused into the filtrate. The product was obtained as 0.022 g (44%) of red crystals. Mass spectrum: *m/z* 997 ($\{M + H^+\}^+$, 100%). Anal. Calcd for $C_{43}H_{40}N_2NiO_2P_2PtS_2$: C, 51.82; H, 4.05; N, 2.81; S, 6.43. Found: C, 51.43; H, 4.02; N, 2.73; S, 6.64. *Method B*: To a solution of $(Et_4N)_2[Ni(L\text{-}655)]$ (0.027 g, 0.05 mmol) in 5 mL of acetonitrile was added a suspension of *trans*-$[Pt(PPh_3)_2Cl_2]$ (0.040 g, 0.05 mmol) in 2 mL of acetonitrile; THF (2 mL) was added, and mixture was stirred for 2 h. The workup procedure of method A was followed. The product was obtained as 0.028 g (56%) of red crystals. Mass spectrum: *m/z* 997 ($\{M + H^+\}^+$, 60%).

(Et_4N)$_3$[Fe_4S_4(LS_3)(bdt)] ((Et_4N)$_3$[17]). To a solution of $(Bu_4N)_2[Fe_4S_4(LS_3)(OTf)]$[31] (0.100 g, 0.051 mmol) in 15 mL of acetonitrile were added a suspension of $Na_2(bdt)$ (0.010 g, 0.051 mmol) in 3 mL of acetonitrile and a solution of Et_4NCl (0.025 g, 0.15 mmol) in 2 mL of acetonitrile. The mixture was stirred for 10 h. A brown-black solid was collected and washed with ether. The product was obtained as 0.058 g (62%) of brown-black solid. ^1H NMR (Me_2SO, anion): δ 10.01 (Ph), 8.35 (5-H), 7.18, 6.61 (2′-H, 3′-H), 4.09, 3.48 (6-Me, 4-Me), 2.27 (4′-Me).

(Bu_4N)[{Ni(L_O-S_2N_2)}Fe_4S_4(LS_3)] ((Bu_4N)[18]). To a solution of $(Bu_4N)_2[Fe_4S_4(LS_3)(OTf)]$ (0.050 g, 0.026 mmol) in 10 mL of acetonitrile was added a solution of $[Ni(L_O\text{-}S_2N_2)]$ (0.008 g, 0.026 mmol) in 2 mL of acetonitrile. The mixture was stirred for 2 h and filtered through Celite. The filtrate was concentrated and ether was layered; a brown-black solid was obtained and washed with ether. The product was obtained as 0.036 g (77%) of brown-black solid. ^1H NMR (CD_3CN, anion): δ 15.42, 12.78 (SCH_2), 8.37 (5-H), 7.16, 6.74 (2′-H, 3′-H), 5.04 (br, 2-H), 4.04, 3.88 (6-Me, 4-Me), 2.26 (4′-Me). Three CH_2 signals and a Me signal occur as multiplets at δ ~1.0 to 2.5.

(Et_4N)$_3$[{Ni(phma)}Fe_4S_4(LS_3)] ((Et_4N)$_3$[19]). To a solution of $(Bu_4N)_2[Fe_4S_4(LS_3)(OTf)]$ (0.097 g, 0.050 mmol) in 10 mL of acetonitrile were added a solution of $(Et_4N)_2[Ni(phma)]$[32] (0.029 g, 0.055 mmol) in 3 mL of acetonitrile and a solution of $(Et_4N)(BF_4)$ (0.012 g, 0.05 mmol) in 2 mL of acetonitrile. The mixture was stirred for 1 h and filtered through Celite. Ether was diffused into the filtrate, affording the product as 0.087 g (87%) of dark black crystals. Mass spectrum: *m/z* 1056.7 ($\{M - H_2LS_3\}^-$, 50%). ^1H NMR (CD_3CN, anion): δ 13.2 (SCH_2), 8.30 (Ph-H), 8.25 (5-H), 7.16, 6.75 (2′-H, 3′-H), 6.49 (Ph-H), 4.86 (br, 2-H), 3.94, 3.68 (6-Me, 4-Me), 2.26 (4′-Me).

X-ray Structure Determinations. Twelve compounds were structurally identified by X-ray crystallography. Diffraction quality crystals were obtained as follows: layering hexanes on a dichloromethane solution, **1** (orange blocks, 1 d); layering ether onto or vapor diffusion of ether into acetonitrile solutions, (Bu_4N)[**2**] (orange blocks), **4** (dark red blocks), [**5**][$Ni(PPh_3)Cl_3$]$_2$ (brown-green plates), [**6**,**7**,**9**,**10**](PF_6) (red plates), (Bu_4N)[**18**]·1.5MeCN·0.5Et_2O (dark brown plates) (all 1−3 d); [**8**](PF_6), **13**·CH_2Cl_2, vapor diffusion of ether in dichloromethane solutions. (Bu_4N)$_3$[**21**]·3MeCN was obtained by the reaction of $(Bu_4N)_2[Fe_4S_4(LS_3)(SEt)]$ with $(Et_3NH)(OTf)$ in acetonitrile, removal of solvent, and crystallization of the solid residue from acetonitrile/ether. Crystals were coated in grease and mounted on a Siemens (Bruker) SMART CCD area detector instrument with Mo Kα radiation. Data were collected at either 193 or 213 K with ω scans of 0.3°/frame, with 30 s/frame (except for (Bu_4N)[**18**]·1.5MeCN·0.5Et_2O, which was collected at 60 s/frame), such that 1271 frames were collected for a hemisphere of data. The first 50 frames were re-collected at the end of the data collection to monitor for decay; no significant decay was found for any compound. Data out to 2θ of 56.7° were used for (Bu_4N)[**2**] and [**6**,**7**,**10**](PF_6) and to 2θ of 50.0° for [**9**](PF_6); for the remaining compounds data out to 2θ of 45° were used because of the low-quality high-angle data. Cell parameters were retrieved using SMART software and refined on all observed reflections between 2θ of 3° and the upper thresholds. Data reduction was performed with SAINT, which corrects for Lorentz polarization and decay. Absorption corrected were applied with SADABS, as described by Blessing.[37] Space groups of all compounds were assigned unambiguously by analysis of symmetry and systematic absences determined by XPREP. Crystal parameters are listed in Table S1.[38]

All structures were solved by direct methods with SHELXS-97 and subsequently refined against all data in the 2θ ranges by full-matrix least squares on F^2. Hydrogen atoms were attached at idealized positions on carbon atoms. The program PLATON was used to check for missing symmetry. Final agreement factors are given in Table S1.[38]

For the compound (Bu_4N)[**18**]·1.5MeCN·0.5Et_2O, there are two independent anions in the asymmetric unit. In one anion, a phenyl ring is disordered over two positions. Solvent molecules are disordered and were refined isotropically. No disorder was evident in any other structure. Crystals of (Et_4N)$_3$[**19**] were obtained by vapor diffusion of ether into an acetonitrile solution. The structure was solved in monoclinic space group $P2_1/n$ with $a = 19.31(1)$ Å, $b = 64.72(4)$ Å, $c = 19.49(1)$ Å, and $\beta = 119.5(1)°$. Because of limited data, the structure was refined to $R_1 = 0.175$ with $2\theta = 45°$. The data are sufficient to demonstrate the overall structure and certain metric features.

Reactions Monitored by ^1H NMR Spectroscopy. A series of binuclear (**6**−**10**) and mononuclear complexes (**2a**,**b**) were reacted with cluster **14** or **15** in CD_3CN, Me_2SO-d_6, or CD_2Cl_2 solution at ambient temperature or over a temperature range. In a typical experiment, the reaction system contained 6−17 mM cluster and an approximately equal concentration of complex. Spectra were measured within 10−20 min after solution preparation with a Varian AM-400B spectrometer.

Other Physical Measurements. All measurements were performed under anaerobic conditions. ^1H NMR spectra were measured with a

---

(30) Brugat, N.; Polo, A.; Álvarez-Larena, A.; Piniella, J. F.; Real, J. *Inorg. Chem.* **1999**, *38*, 4829−4837.

(31) Zhou, J.; Hu, Z.; Münck, E.; Holm, R. H. *J. Am. Chem. Soc.* **1996**, *118*, 1966−1980. In a matter relevant to this work, footnote 53 in the cited work points out that the cluster formulated as $[Fe_4S_4(LS_3)(OTf)]^{2-}$ may actually be $[Fe_4S_4(LS_3)(solv)_x]^-$ in a donor solvent. In either formulation, the unique site is certain to be more activated toward substitution than the site in **15**. The triflate formulation is retained here.

(32) Krüger, H.-J.; Peng, G.; Holm, R. H. *Inorg. Chem.* **1991**, *30*, 734−743.

(33) Krüger, H.-J.; Holm, R. H. *Inorg. Chem.* **1989**, *28*, 1148−1155.

(34) Schneider, J.; Hauptmann, R.; Osterloh, F.; Henkel, G. *Acta Crystallogr.* **1999**, *C55*, 328−330.

(35) Stack, T. D. P.; Holm, R. H. *J. Am. Chem. Soc.* **1988**, *110*, 2484−2494.

(36) Ciurli, S.; Carrié, M.; Weigel, J. A.; Carney, M. J.; Stack, T. D. P.; Papaefthymiou, G. C.; Holm, R. H. *J. Am. Chem. Soc.* **1990**, *112*, 2654−2664.

(37) Blessing, R. H. *Acta Crystallogr.* **1995**, *A51*, 33−38.

(38) See paragraph at the end of this article for Supporting Information Available.

Scheme 1. Synthesis of Bridged Complexes with Appended Fe^{II} (**4**), Ni^{II} (**5**, **8**), Pd^{II} (**6**, **9**), and Pt^{II} (**7**, **10**) Units from Precursor Ni^{II} Complex **3** by the Formation of Nonplanar Ni(μ_2-SR)$_2$M Rhombs

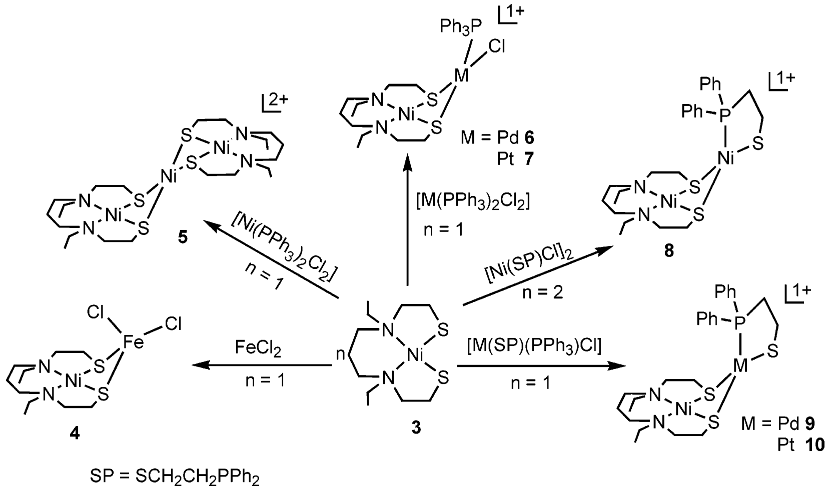

Scheme 2. Formation of Bridged Ni^{II} (**12**) and Pt^{II} (**13**) Complexes from Precursor Ni^{II} Complex **11** by Means of Ni(μ_2-SR)$_2$M^{II} Rhombs

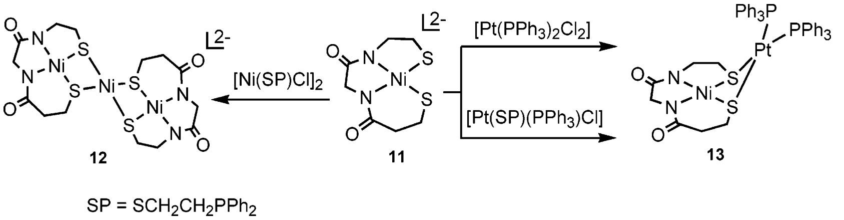

Varian AM-400B spectrometer. Electrospray mass spectra were recorded on a Platform II quadrupole mass spectrometer (Micromass Instruments, Danvers, MA) or on an LCT-TOF mass spectrometer (Micromass Instruments, Danvers, MA).

Results and Discussion

Step (iii) is ideally represented by minimal reaction 1, in which a nickel- or other metal-bound terminal thiolate forms a single unsupported bridge to an Fe_4S_4 cluster. Components of the reaction systems are first considered, followed by a discussion of real or potential bridging reactions themselves.

$$[Fe_4S_4]^{2+} + M^{II}{-}SR \rightarrow [Fe_4S_4]^{2+}{-}(\mu_2\text{-SR}){-}M^{II} \quad (1)$$

Design of Reaction Systems. (a) Clusters. The site of binding of the nickel thiolate moiety on the Fe_4S_4 portion of the A-cluster is differentiated by protein structure. Here that situation is simulated by the use of 3:1 site-differentated clusters **14** and **15** supported by the semirigid tridentate cavitand ligand LS_3.[39] These clusters sustain regiospecific substitution reactions at the unique site, as illustrated by generalized reaction 2, in which the original ligand is itself a potential bridging ligand (L′ = SEt) or is readily displaced by a donor solvent or an incoming ligand (L′ = TfO$^-$).[31] Product formation is indicated from the pronounced sensitivity of some or all of the 4-Me, 5-H, and 6-Me ^{1}H isotropic shifts to the identity of the ligand at the unique site.[20,36,40,41] Representative examples of reaction 2 have been summarized.[42]

$$[Fe_4S_4(LS_3)L']^{2-} + X^z \rightarrow [Fe_4S_4(LS_3)X]^{(1-)+z} + (L')^- \quad (2)$$

(b) Dinuclear Metal Reactants. These species contain Ni(μ_2-SR)$_2$M bridge rhombs with potentially displaceable ligands bound to M = Pd^{II}/Pt^{II} (**6**, **7**) or an M−SR group as part of a ring structure with M = Ni^{II}/Pd^{II}/Pt^{II} (**8**−**10**). Preparations of reactant complexes are summarized in Schemes 1 and 2. Structures of selected molecules are provided in Figures 2 and 3, together with metric parameters of coordination units.

Dinuclear reactants are based on planar complex **3**,[26] selected because its S−Ni−S angle of 84.2° [34] is favorable for closing a Ni(μ_2-SR)$_2$M ring[17] and also because its 5−6−5 chelate ring pattern is symmetrical, a property advantageous to ^{1}H NMR examination of reaction products. This complex binds Fe^{II}, Ni^{II}, Pd^{II}, and Pt^{II}, thus providing further examples of stable molecules with Ni^{II}(μ_2-SR)$_2$M^{II} bridge rhombs (Scheme 1). Complex **4** (Ni^{II}Fe^{II}) demonstrates the ability to bind Fe^{II} in a tetrahedral environment that is highly distorted, primarily by the S−Fe−S angle of 72.7(1)° which is inflicted by the S−Ni−S bite angle of 82.1(1)° and pyramidal stereochemistry at the sulfur atoms (Figure 2). Complexes **6** (Ni^{II}Pd^{II}) and **7** (Ni^{II}Pt^{II}), obtained by the reaction of **3** with [M(PPh$_3$)$_2$Cl$_2$], contain potentially replaceable ligands at their planar Pd^{II} and Pt^{II} sites (Figure 3). Attempts to prepare the binuclear Ni^{II}Ni^{II} complex by an analogous reaction afforded instead green trinuclear **5**, whose linear Ni$_3$ arrangement (Figure 2) is frequently formed when attempting to prepare thiolate species of lower nuclearity. Trinuclear bridged Ni^{II}−S$_2$N$_2$ complexes are now commonly encountered.[18,43−49] Complexes **9** (Ni^{II}Pd^{II}) and **10** (Ni^{II}Pt^{II}) are readily formed by displacement of unidentate ligands from

---

(39) Stack, T. D. P.; Weigel, J. A.; Holm, R. H. *Inorg. Chem.* **1990**, *29*, 3745−3760.
(40) Weigel, J. A.; Holm, R. H. *J. Am. Chem. Soc.* **1991**, *113*, 4184−4191.
(41) Zhou, C.; Holm, R. H. *Inorg. Chem.* **1997**, *36*, 4066−4077.
(42) Venkateswara Rao, P.; Holm, R. H. *Chem. Rev.* **2004**, *104*, 527−559.
(43) Wei, C. H.; Dahl, L. F. *Inorg. Chem.* **1970**, *9*, 1878−1887.
(44) Barrera, H.; Suades, J.; Perucaud, M. C.; Briansó, J. L. *Polyhedron* **1984**, *3*, 839−843.
(45) Turner, M. A.; Driessen, W. L.; Reedijk, J. *Inorg. Chem.* **1990**, *29*, 3331−3335.

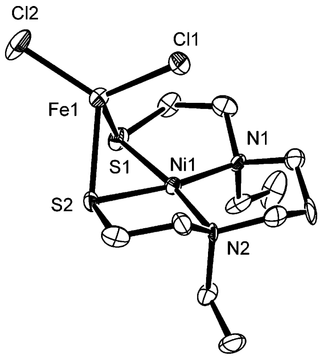

$[\{\mathrm{Ni(L_{O}\text{-}S_2N_2)}\}\mathrm{FeCl_2}]$

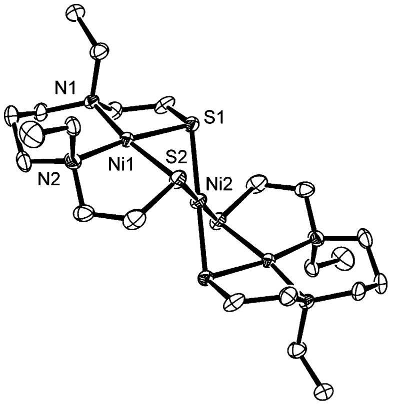

$[\{\mathrm{Ni(L_{O}\text{-}S_2N_2)}\}_2\mathrm{Ni}]^{2+}$

Figure 2. Structures of the Ni^{II}Fe^{II} complex **4** (upper) and the trinuclear centrosymmetric Ni^{II} complex **5** (lower). In this and other X-ray structural figures, 50% probability ellipsoids and partial atom labeling schemes are shown. Selected (mean) dimensions: for **4**, Ni−N 1.989(8) Å, Ni−S1 2.177(3) Å, Ni−S2 2.188(2) Å, Fe−S1 2.426(3) Å, Fe−S2 2.410(3) Å, S1−Ni−S2 82.1(1)°, S1−Fe−S2 72.7(1)°; for **5**, Ni−N 1.979(4) Å, Ni1−S 2.170(2) Å, Ni2−S 2.208(1) Å, S1−Ni1−S2 81.27(5)°, S1−Ni2−S2 79.59(5)°.

[M(SCH$_2$CH$_2$PPh$_2$)(PPh$_3$)Cl]. The Pd^{II} complex used in the synthesis of **9** has been reported;[30] Pt^{II} complex **1** was prepared and structurally characterized (Figure 4) as a precursor to **10**. Complex **8** (Ni^{II}Ni^{II}) could not be prepared by a similar method but was obtained by cleavage of dinuclear [Ni$_2$(Ph$_2$PCH$_2$CH$_2$(μ_2-S))$_2$Cl$_2$] by **3**. Less extensive experimentation with unsymmetrical **11** as the basis complex afforded previously prepared trinuclear **12**[17] and a new species, **13** (Ni^{II}Pt^{II}, Figure 3), obtainable by two procedures. All attempts to synthesize dinculear complexes analogous to **8**−**10** from **11** did not yield tractable materials. Reactions intended to form Ni^{II}Ni^{II} complexes gave **12** instead. Members of the set **5**−**10** have the common features of nonplanar Ni^{II}−(μ_2-SR)$_2$−M^{II} bridge rhombs folded by 107−118° along the S···S direction and planar coordination sites.

(c) Mononuclear Metal Reactants. The thiolate complex [Ni(pdmt)(SEt)]$^-$ (**2a**) was reported previously.[33] The corresponding Pd^{II} complex **2b** has been prepared in an analogous manner by cleavage of dinuclear [Pd$_2$(pdmt)$_2$] with ethanethiolate (Scheme 3). It is planar and isostructural with [Ni(pdmt)(SEt)]$^-$ (Figure 4). These molecules present a highly basic alkylthiolate ligand in a sterically unimpeded position. Attempts to prepare the corresponding Pt^{II} complex by thiolate cleavage of [Pt$_2$(pdmt)$_2$][28] were unsuccessful. The dinuclear structures proposed for the Ni^{II} and Pd^{II} complexes by ourselves[33] (Scheme 3) and others[28] follow by analogy from proven structures of dinuclear Ni^{II} complexes with five-membered

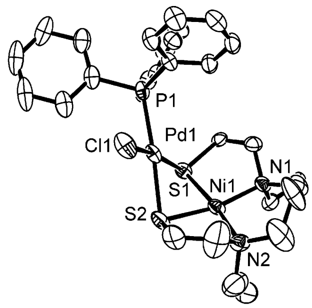

$[\{\mathrm{Ni(L_{O}\text{-}S_2N_2)}\}\mathrm{Pd(PPh_3)Cl}]^{1+}$

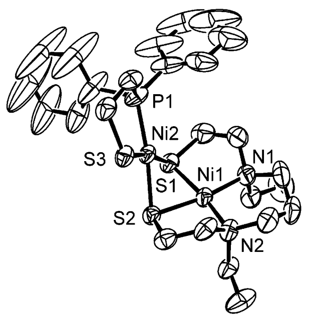

$[\{\mathrm{Ni(L_{O}\text{-}S_2N_2)}\}\mathrm{Ni(SCH_2CH_2PPh_2)}]^{1+}$

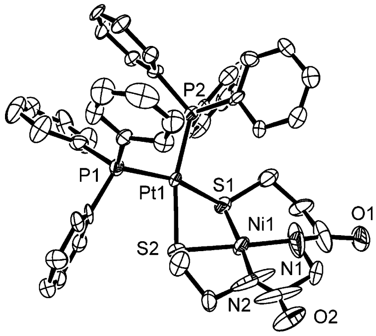

$[\{\mathrm{Ni(L\text{-}655)}\}\mathrm{Pt(PPh_3)_2}]$

Figure 3. Structures of the Ni^{II} Pd^{II} complex **6** (upper), Ni^{II}Ni^{II} complex **8** (middle), and Ni^{II}Pt^{II} complex **13** (lower). Complex **7** is isostructural with **6**, and complexes **9** and **10** are isostructural with **8**. Selected (mean) dimensions: for **6**, Ni−N 1.991(5) Å, Ni−S1 2.184(2) Å, Ni−S2 2.160(2) Å, Pd−S 2.325(2) Å, Pd−Cl 2.310(2) Å, Pd−P 2.282(2) Å, S1−Ni−S2 81.87(7)°, S1−Pd−S2 75.48(6)°; for **7**, Ni−N 1.989(7) Å, Ni−S1 2.190(2) Å, Ni−S2 2.165(3) Å, Pt−S1 2.282(3) Å, Pt−S2 2.358(2) Å, Pt−Cl 2.321(2) Å, Pt−P 2.257(2) Å, S1−Ni−S2 81.51(9)°, S1−Pt−S2 75.54(8)°; for **8**, Ni−N 1.977(6) Å, Ni1−S 2.158(2) Å, Ni2−S1 2.229(2) Å, Ni2−S2 2.229(2) Å, Ni2−S3 2.156(2) Å, Ni2−P 2.142(2) Å, S1−Ni1−S2 80.32(7)°, S1−Ni2−S2 77.25(7)°, P−Ni2−S3 87.70(7)°; for **9**, Ni−N 1.991(7) Å, Ni−S 2.176(3) Å, Pd−S1 2.364(2) Å, Pd−S2 2.360(2) Å, Pd−S3 2.278(2) Å, Pd−P 2.230(2) Å, S1−Ni−S2 81.79(9)°, S1−Pd−S2 74.17(8)°, P−Pd−S3 86.34(8)°; for **10**, Ni−N 1.981(7) Å, Ni−S 2.181(2) Å, Pt−S1 2.364(2) Å, Pt−S2 2.354(2) Å, Pt−S3 2.283(2) Å, Pt−P 2.228(2) Å, S1−Ni−S2 81.41(9)°, S1−Pt−S2 74.17(7)°, P−Pt−S3 86.83(8)°; for **13**, Ni−N 1.85(2) Å, Ni−S 2.15(1) Å, Pt−S 2.368(4) Å, Pt−P 2.29 (1) Å, Ni···Pt 3.077(2) Å, S−Ni−S 84.1(2)°, S−Pt−S 74,8(1)°.

---

(46) Farmer, P. J.; Solouki, T.; Mills, D. K.; Soma, T.; Russell, D. H.; Reibenspies, J. H.; Darensbourg, M. Y. *J. Am. Chem. Soc.* **1992**, *114*, 4601−4605.

(47) Golden, M. L.; Jeffery, S. P.; Miller, M. L.; Reibenspies, J. H.; Darensbourg, M. Y. *Eur. J. Inorg. Chem.* **2004**, 231−236.

(48) Hatlevik, O.; Blanksma, M. C.; Mathrubootham, V.; Arif, A. M.; Hegg, E. L. *J. Biol. Inorg. Chem.* **2004**, *9*, 238−246.

(49) Golden, M. L.; Rampersad, M. V.; Reibenspies, J. H.; Darensbourg, M. Y. *Chem. Commun.* **2003**, 1824−1826.

Table 1. Chemical Shifts of $[Fe_4S_4(LS_3)]$ Clusters

			δ			
	solvent	*T* (K)	SCH_2	5-H	6-Me, 4-Me	ref
$[Fe_4S_4(LS_3)(SEt)]^{2-}$ (**15**)	CD_3CN	296	13.20	8.15	3.82, 3.69	23
	CD_2Cl_2	296	13.06	8.04	3.87, 3.76	*a*
		273	12.32	7.95	3.71^b	
		243	11.13	7.80	3.61, 3.46	
$[Fe_4S_4(LS_3)(SBu^t)]^{2-}$	CD_3CN			8.12	3.80, 3.65	35
$[Fe_4S_4(LS_3)(SPh)]^{2-}$	$Me_2SO\text{-}d_6$			8.13	3.85, 3.65	36
$[\{Fe_4S_4(LS_3)\}_2S]^{4-}$	CD_3CN	296		8.66	4.53, 4.09	23
$[Fe_4S_4(LS_3)(OTf)]^{2-}$ (**14**)	CD_3CN	296		8.25	3.93^b	
	$Me_2SO\text{-}d_6$	296		8.12	3.84, 3.57	*a*
$[Fe_4S_4(LS_3)Cl]^{2-}$ (**16**)	CD_3CN	296		8.24	3.88^b	
	$Me_2SO\text{-}d_6$	296		8.22	3.91, 3.80	*a*
	CD_2Cl_2	296		8.13	3.92^b	*a*
$[Fe_4S_4(LS_3)(bdt)]^{3-}$	$Me_2SO\text{-}d_6$	296		8.32	4.06, 3.46	36
$[Fe_4S_4(LS_3)(tdt)]^{3-}$	$Me_2SO\text{-}d_6$	296		8.33	4.08, 3.47	36
$[\{Ni(phma)\}Fe_4S_4(LS_3)]^{3-}$	CD_3CN	296	13.32	8.25	3.94, 3.68	*a*
$[\{Ni(L_o\text{-}S_2N_2)\}Fe_4S_4(LS_3)]^{-}$	CD_3CN	296	15.42, 12.78	8.37	4.04, 3.88	
$[Fe_4S_4(LS_3)(OTf)]^{2-}$/ $[Ni(pdmt)(SEt)]^{-}$ (**20**)	CD_2Cl_2	296	13.35	8.11	3.89, 3.71	*a*
		273	12.66	8.03	3.75, 3.65	
		243	11.38	7.87	3.59, 3.50	
	$+ CD_3CN^c$	296	13.13	8.06	3.78, 3.67	*a*
	CD_3CN	296	13.22	8.16	3.83, 3.69	*a*
		273	12.51	8.10	3.71, 3.63	
		243	11.14	7.96	3.48^b	
	$Me_2SO\text{-}d_6$	296	13.01	8.12	3.83, 3.57	
$[Fe_4S_4(LS_3)(OTf)]^{2-}$/ $[Pd(pdmt)(SEt)]^{-}$	CD_3CN	296	13.21	8.15	3.83, 3.70	*a*
	$Me_2SO\text{-}d_6$	296	13.08	8.12	3.84, 3.58	*a*
	$CD_2Cl_2^d$	296	13.01	8.03	3.92, 3.75	
		273	12.32	7.94	3.76, 3.70	
		243	11.10	7.79	3.61, 3.45	

[a] This work. [b] One signal observed. [c] Added to CD_2Cl_2 solution; 3:7 v/v CD_3CN/CD_2Cl_2. [d] Shifts identical to those of $[Fe_4S_4(LS_3)(SEt)]^{2-}$ at 213−296 K.

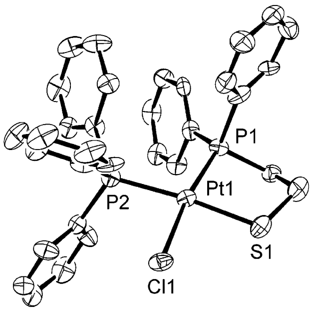

$[Pt(SCH_2CH_2PPh_2)(PPh_3)Cl]$

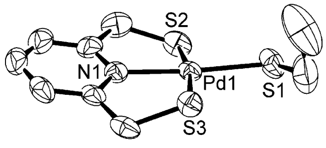

$[Pd(pdmt)SEt]^{1-}$

Figure 4. Structures of Pt^{II} complex **1** (upper) and Pd^{II} complex **2b** (lower). Selected dimensions: for **1**, Pt−P1 2.215(4) Å, Pt−P2 2.281(4) Å, Pt−Cl1 2.362(4) Å, Pt−S1 2.319(3) Å; for **2b**, Pd−N1 2.035(3) Å, Pd−S1 2.284(1) Å, Pd−S2 2.304(1) Å, Pd−S3 2.305(1) Å, S2−Pd−S3 170.56(4)°, S1−Pd−S2 90.52(5)°, S1−Pd−S3 98.68(4)°.

aminodithiolate chelate rings[50,51] and the mass spectrometric observation of the dinuclear parent ion of the Ni^{II} complex.[52]

Scheme 3. Synthesis of Pt^{II} Complex **1**, Ni^{II} Complex **2a**, and Pd^{II} Complex **2b**

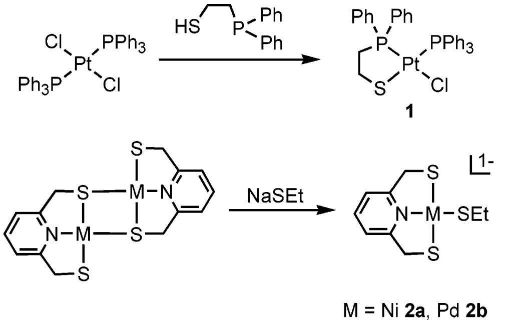

Reactions of Dinuclear Complexes. Reactions of clusters **14** and **15** and complexes **6**−**10** were examined in situ by ^1H NMR spectroscopy in homogeneous solutions. Chemical shifts useful for cluster identification in these and other reaction systems are collected in Table 1. Results are summarized in Scheme 4; note the substituent numbering of the LS_3 ligand. The 5-H signal in particular is very sharp and sensitive to the ligand at the unique site. It is well established that ^1H NMR resonances of $[Fe_4S_4]^{2+}$ clusters are isotropically (paramagnetically) shifted by dominant contact interactions arising from thermal occupancy of an excited $S = 1$ state. The isotropic components of the chemical shifts decrease with decreasing temperature owing to reduced population of the triplet state.[53]

Treatment of thiolate cluster **15** with **6** or **7** potentially could result in displacement of phosphine and/or chloride and the development of the desired Fe−(μ_2-SEt)−M bridge. However, reactions in Me_2SO solutions afforded the same major product;

---

(50) Colpas, G. J.; Kumar, M.; Day, R. O.; Maroney, M. J. *Inorg. Chem.* **1990**, *29*, 4779−4788.

(51) Choudhury, S. B.; Pressler, M. A.; Mirza, S. A.; Day, R. O.; Maroney, M. J. *Inorg. Chem.* **1994**, *33*, 4831−4839.

(52) Constable, E. C.; Lewis, J.; Marquez, V. E.; Raithby, P. R. *J. Chem. Soc., Dalton Trans.* **1986**, 1747−1749.

(53) Reynolds, J. G.; Laskowski, E. J.; Holm, R. H. *J. Am. Chem. Soc.* **1978**, *100*, 5315−5322.

Scheme 4. Formation of 3:1 Site-Differentiated Clusters with Four- or Five-Coordinate Unique Sites by Ligand Substitution (**16**, **17**), Binding of Ni^{II}−S$_2$N$_2$ Complexes (**18**, **19**), or Cleavage of Dinuclear Complexes (**18**)[a]

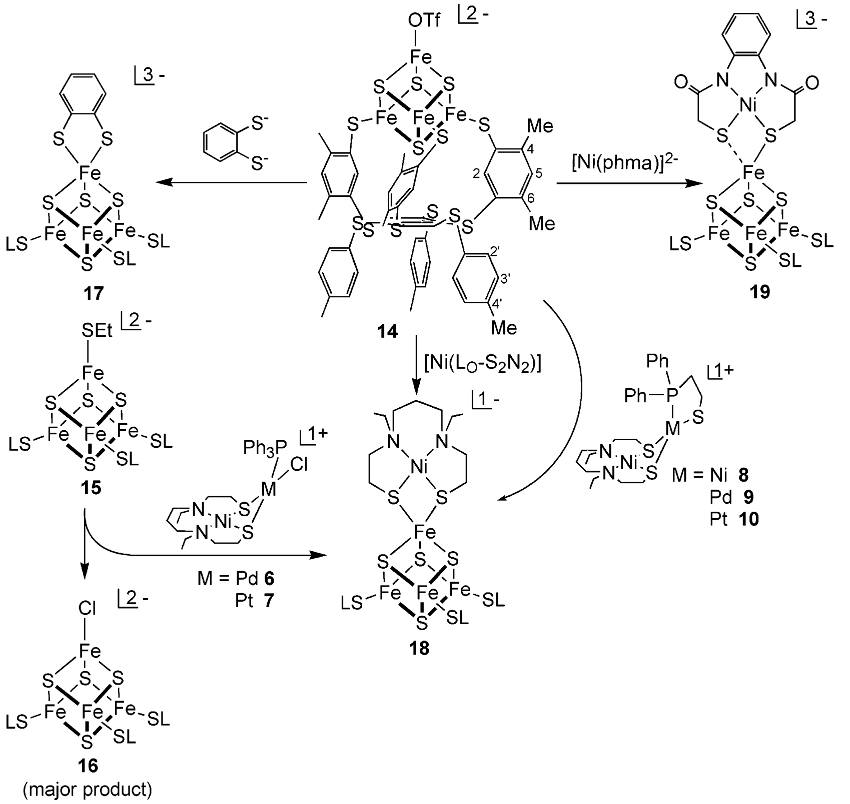

[a] Cluster **16** is the major product in the reaction of **15** with **6**/**7**. The bridging interactions in **19** are highly unsymmetrical. Note the LS$_3$ numbering scheme in **14**; 3LS = LS$_3$ in **15**−**19** and in Scheme 5.

none of the initial cluster remained. The product spectrum is identical to that of chloride cluster **16**, whose structure has been determined.[35] In these systems, chloride replaces thiolate in proposed reaction 3. Thiolate is fully transferred to the softer

$$[\mathrm{Fe_4S_4(LS_3)(SEt)}]^{2-} + [\{\mathrm{Ni(L_O\text{-}S_2N_2)}\}\mathrm{M(PPh_3)Cl}]^{+} \rightarrow [\mathrm{Fe_4S_4(LS_3)Cl}]^{2-} + [\{\mathrm{Ni(L_O\text{-}S_2N_2)}\}\mathrm{M(PPh_3)(SEt)}]^{+} \quad (3)$$

metal center rather than forming a bridge. Systems initially containing triflate cluster **14** with complexes **8**, **9**, or **10** in dichloromethane, in which the potential proximal metal site is bound to a putative μ_2-SR group in a ring structure, resulted in the same major product **18** in each case, recognized by two equally intense downfield signals (δ 12.78, 15.42). Additionally, the 5-H shift (δ 8.37) does not correspond to any known cluster in this solvent. The identity of the product was suggested by a similarity to the spectrum of the 2:2 site-differentiated cluster [{Ni(L$_O$-S$_2$N$_2$)}$_2$Fe$_4$S$_4$I$_2$] (δ 16.76, 18.96 in CD$_2$Cl$_2$) obtained from the reaction of 2 equiv of [Ni(L$_O$-S$_2$N$_2$)] and 1 equiv of [Fe$_4$S$_4$I$_4$]$^{2-}$, and its thiolate substitution product [{Ni(L$_O$-S$_2$N$_2$)}$_2$-Fe$_4$S$_4$(Stibt)$_2$] (δ 12.76, 15.26 in CDCl$_3$).[26] These signals arise from the SCH$_2$ group of complex **3**, bound as a bidentate ligand at two iron sites of the [Fe$_4$S$_4$]$^{2+}$ core. Small amounts of **18** were also detected in the reactions of **15** with **6** or **7**.

Identification of the preceding reaction product was sought by means of reaction 4 in acetonitrile. The product of this

$$[\mathrm{Fe_4S_4(LS_3)(OTf)}]^{2-} + [\mathrm{Ni(L_O\text{-}S_2N_2)}] \rightarrow [\{\mathrm{Ni(L_O\text{-}S_2N_2)}\}\mathrm{Fe_4S_4(LS_3)}]^{-} + \mathrm{TfO}^{-} \quad (4)$$

reaction was isolated as the black Bu$_4$N$^+$ salt in 77% yield. With reference to Figure 5A−C, the ^{1}H NMR spectrum of this material (5C) is different from that of initial cluster **14** (5A) and displays a 5-H shift (δ 8.37), characteristic of a five-coordinate FeS$_5$ site as in **17** and related clusters,[36] and two SCH$_2$ signals (δ 12.78, 15.42). The identity of the product was established by an X-ray structure determination. The solvated Bu$_4$N$^+$ salt of cluster **18** crystallizes with two crystallographically independent anions whose structures are very similar. The overall structure of **18** is set out in Figure 6; more detailed views of the individual clusters are provided in Figure 7. Metric features are summarized in Table 2. The essential structural features of clusters bound by the trigonal semirigid cavitand ligand LS$_3$ have been analyzed previously.[39] The cluster has the *ababab* conformation in which the three *p*-tolylthio groups are the same side of the central benzene ring, opposite the coordinating arms. The most prominent feature is the five-coordinate iron site, at which [Ni(L$_O$-S$_2$N$_2$)] is bridged to the [Fe$_4$S$_4$]$^{2+}$ core by means of nonplanar Ni(μ_2-SR)$_2$Fe rhombs with dihedral angles of 99.0° and 100.9° between the FeS$_2$ and mean NiS$_2$N$_2$ planes. The fold along the S···S direction positions the nickel atom above the Fe1−S3 and Fe5−S16 core edges of the two clusters, at the nonbonding distances of 3.16 Å from S3 and 3.34 Å from S16. The coordination geometry at the unique iron sites is highly irregular but can be conceptualized as a distorted square pyramid. Taking cluster 1 as an example, the angles S3−Fe1−S1,2,5,6 occur in the range 101.6(1)−112.6(2)°; the two largest S−Fe−S angles, S1−Fe1−S5 = 141.0(2)° and S2−Fe1−S6 = 149.1(2)°, define the equatorial sulfur atoms and relegate S3 to the axial position. The iron atom is

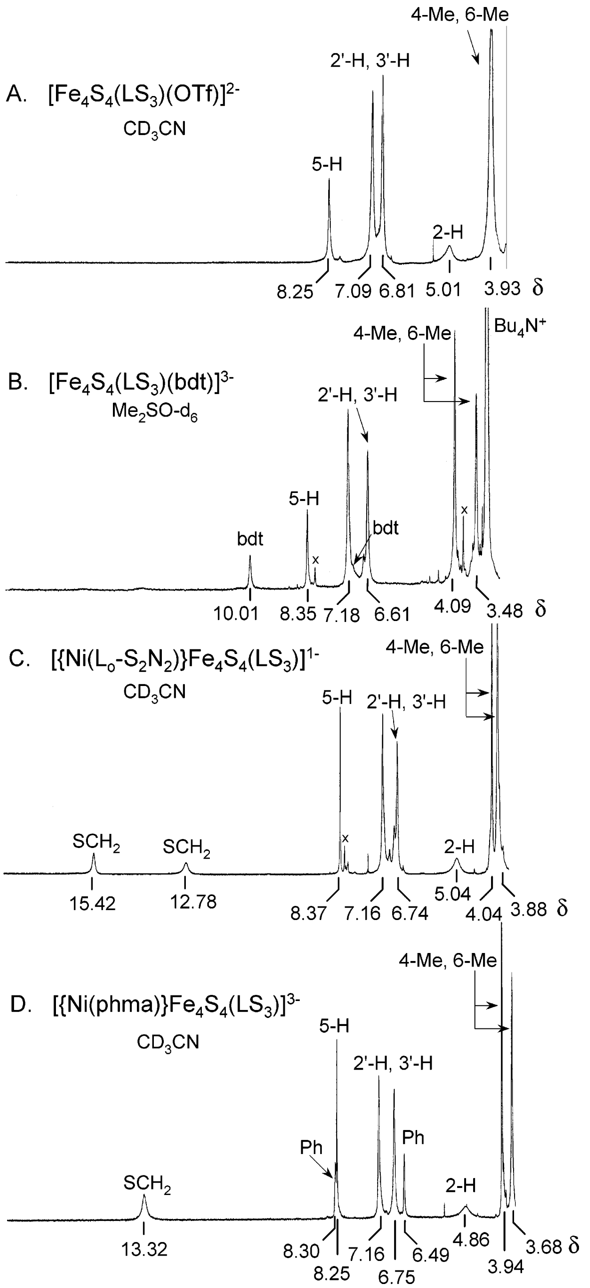

Figure 5. ^{1}H NMR spectra of clusters **14** (A), **17** (B), **18** (C), and **19** (D). In this and subsequent NMR figures, spectra refer to 298 K, solvents and signal assignments are indicated, and x = impurity.

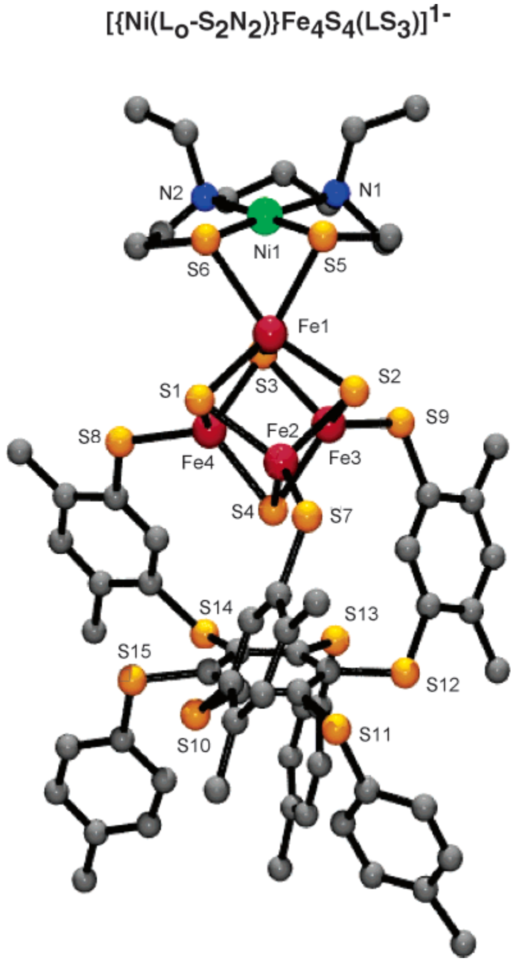

Figure 6. Structure of cluster **18** showing the entire anion. The asymmetric unit contains two inequivalent clusters with very similar structures. One cluster is shown in a ball-and-stick presentation for clarity.

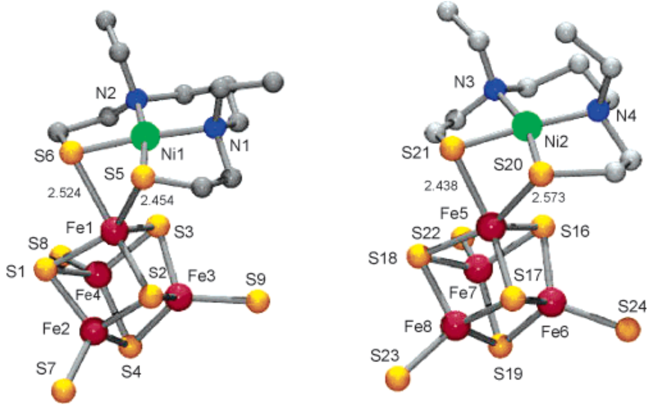

Figure 7. Structures of the two inequivalent clusters of **18**, with Fe−S bond lengths (Å) in the bridging rhombs.

displaced 0.62 Å in the direction of S3. Equatorial bond angles are 65.0(2)° and 89.9(2)−98.3(2)°, with the smallest angle in the bridging rhomb. Axial−equatorial bond angles define the range 103.0(1)−112.6(2)°. The Fe(μ_2-SR)$_2$Ni bridge rhomb differs from that in **4** most notably because of unsymmetrical Fe−SR coordination. Bond lengths differ by 0.07 and 0.13 Å in the two clusters, with the longer distances of 2.524(6) and 2.573(5) Å representing weak interactions (Figure 7). Core Fe−S bonds opposite the two Fe−SR bonds occur in the 2.32−2.37 Å interval, compared to the mean value of 2.27(2) Å for all other core bonds, reflecting a trans influence of the μ_2-SR ligands in the five-coordinate sites. The disposition of the two ethyl groups on the same side of the NiS$_2$N$_2$ coordination plane differentiates the SCH$_2$ protons, accounting for two isotropically shifted resonances. Overall, the structure of **18** is similar to those of the clusters reported by Osterloh et al.,[26] but differs by binding one complex **3** owing to its site-differentiated nature. A preliminary structure of [{Ni(L$_O$-S$_2$N$_2$)}Fe$_4$S$_4$I$_3$]$^-$, obtained with low-quality data from a synthesis described as being of poor reliability, has been communicated.[25]

The possibility of other clusters similar to **18** was pursued by the reaction of **14** with the planar bis(amidatethiolate) complex [Ni(phma)]$^{2-}$.[32] Black (Et$_4$N)$_3$[**19**] was isolated in 87% yield. The structure of cluster **19** (Scheme 4) has been determined but not at a level of accuracy appropriate for a

Table 2. Selected Bond Distances (Å) and Angles (deg) for $[\{Ni(L_O\text{-}S_2N_2)\}Fe_4S_4(LS_3)]^-$ and $[\{Fe_4S_4(LS_3)\}_2(SEt)]^{3-}$

$[\{Ni(L_O\text{-}S_2N_2)\}Fe_4S_4(LS_3)]^-$ (**18**)

		cluster 1		cluster 2	
bridge					
Ni−S		2.173(7)^{b}	2.129(5)^{c}	2.136(7)^{d}	2.166(6)^{e}
Fe−S		2.454(5)^{b}	2.524(6)^{c}	2.573(5)^{d}	2.438(6)^{e}
Ni−Fe		2.819(3)		2.911(3)	
Ni−S−Fe		74.8(2)^{b}	74.1(2)^{c}	75.7(2)^{d}	78.2(2)^{e}
S−Ni−S		76.5(4)		79.4(3)	
S−Fe−S		65.0(3)		66.6(2)	
FeS_2/NiS_2N_2		99.0(2)		100.1(2)	
terminal					
Fe−S(LS_3)^{a}	mean of 3	2.255(9)^{h}		2.256(1)^{i}	
core					
Fe−S		2.332(4)^{f}	2.345(4)^{f}	2.317(4)^{g}	2.374(4)^{g}
	range of 10	2.243(4)−2.294(4)^{h}		2.254(4)−2.294(4)^{i}	
	mean of 10	2.27(2)		2.27(2)	
Fe−Fe	range of 3	2.780(2)−2.887(2)^{j}		2.799(2)−2.914(3)^{k}	
	range of 3	2.705(3)−2.770(2)^{h}		2.719(3)−2.769(3)^{i}	

$[\{Fe_4S_4(LS_3)\}_2(SEt)]^{3-}$ (**21**)

		cluster 1		cluster 2	
bridge					
Fe−S^{a}		2.307(3)		2.316(3)	
Fe−S−Fe		119.70(11)		123.21(13)	
Fe⋯Fe		3.999(2)		4.074(2)	
terminal					
Fe−S(LS_3)^{a}	mean of 6	2.252(9)^{h,i}		2.255(9)^{l,m}	
core					
Fe−S		4 at 2.255(8)^{i,k}	4 at 2.24(1)^{h,j}	4 at 2.253(8)^{l,n}	4 at 2.24(1)^{m,o}
		4 at 2.283(6)^{i,k}	8 at 2.31(1)^{h,j}	4 at 2.29(1)^{l,n}	8 at 2.315(7)^{m,o}
		4 at 2.320(3)^{i,k}		4 at 2.319(6)^{l,n}	
Fe−Fe	range	2.677(2)−2.786(2)^{h,j}		2.705(2)−2.754(2)^{l,n}	
	mean of 6	2.73(4)^{h,j}		2.73(2)^{l,n}	
	range	2.726(2)−2.768(2)^{i,k}		2.671(2)−2.756(2)^{m,o}	
	mean of 6	2.74(2)^{i,k}		2.73(3)^{m,o}	

[a] Mean values. [b] S5. [c] S6. [d] S20. [e] S21. [f] Fe1−S2,3. [g] Fe5−S17,18. [h] Fe2,3,4. [i] Fe6,7,8. [j] Fe1. [k] Fe5. [l] Fe10,11,12. [m] Fe14,15,16. [n] Fe9. [o] Fe13.

detailed description because of limited data. However, the compound has been found to have two clusters in the asymmetric unit with the same overall structure as **18**. $[Ni(phma)]^{2-}$ is coordinated at the unique iron site in a highly unsymmetrical binding mode (Fe−SR = 2.39(1) and 2.64(1) Å in one cluster and 2.45(1) and 2.61(1) Å in the other). Although five-coordinate 3:1 site-differentiated Fe_4S_4 clusters have been previously isolated,[20,36] **18** and **19** are the first such clusters whose structures have been determined. These structures are related to those of $[\{Ni(L_O\text{-}S_2N_2)\}Fe_4S_4I_3]^-$ and $[\{Ni(L_O\text{-}S_2N_2)\}_2Fe_4S_4L_2]$ ($L = I^-$, 2,4,6-$Pr^i{}_3C_6H_2S^-$) described earlier by Osterloh et al.[25,26] Core and bridge rhomb dimensions are comparable to those reported here. Coordination at the unique site is symmetrical in the first iodide cluster cited (Fe−SR = 2.519(8) and 2.536(9) Å) and nearly so in the second iodide cluster (Fe−SR = 2.464(2) and 2.533(2) Å). However, in the thiolate cluster the sites binding the complex are essentially four-coordinate because of one very long Fe⋯SR separation in each (2.812(5) and 2.941(5) Å). The cause of such markedly unsymmetrical binding is not clear. In acetonitrile solution, the inequivalent Fe−S interactions in **19** are averaged, as indicated by a single SCH_2 signal at δ 13.32 in Figure 5D. The 5-H resonance at δ 8.25 implies FeS_4 coordination at the unique site (Table 1). The single methylene signal of **19** (averaged C_{2v} symmetry) is consistent with the explanation of two such signals in **18** (limiting C_s symmetry).

In summary, reactions of dinuclear metal complexes with **14** or **15**, set out in Scheme 4, result in (i) thiolate transfer from the cluster to the reactant (**6**, **7**) or (ii) cleavage of the bridge rhomb and transfer of complex **3** to the cluster (**8**−**10**). It is perhaps ironic that Pd^{II} and Pt^{II} were introduced before the fact to stabilize the dinuclear structure, yet their complexes are as readily cleaved under the conditions tested as is the $Ni^{II}Ni^{II}$ complex **8**. With these results in hand, attention was directed to mononuclear systems containing Ni^{II} or Pd^{II} thiolate complexes where outcome (ii) is obviated but outcome (i) is not.

Reactions of Mononuclear Complexes. The reactions of triflate cluster **14** with complexes **2a**,**b** were examined in acetonitrile, Me_2SO, and dichloromethane solutions. Products are depicted in Scheme 5. The following five reaction systems gave equivalent results: **2a** and **2b** in Me_2SO and acetonitrile and **2b** in dichloromethane. Outcome (i) of these systems is readily conveyed by the ^1H NMR spectrum of the equimolar **2b**/**14** in Me_2SO, provided in Figure 8 and generalized by thiolate transfer reaction 5. The sole cluster product is thiolate

$$[Fe_4S_4(LS_3)(OTf)]^{2-} + [M(pdmt)(SEt)]^- \rightarrow [Fe_4S_4(LS_3)(SEt)]^{2-} + {}^1/_2[M_2(pdmt)_2] + TfO^- \quad (5)$$

cluster **15**, identified by its SCH_2 (δ 13.08) and 5-H (δ 8.12) resonances. The dinuclear Pd^{II} complex (Scheme 3) is ascertained by its methylene signal (δ 4.24), identical with the spectrum of an authentic sample. Formation of $[Ni_2(pdmt)_2]$ in other systems is evident by methylene chemical shifts (e.g., δ 3.59 and 3.91 in Me_2SO). In acetonitrile, the reaction is driven in part by the sparing solubility of the dinuclear product; however, in Me_2SO or dichloromethane, the compound is completely soluble under the conditions used. It is implausible

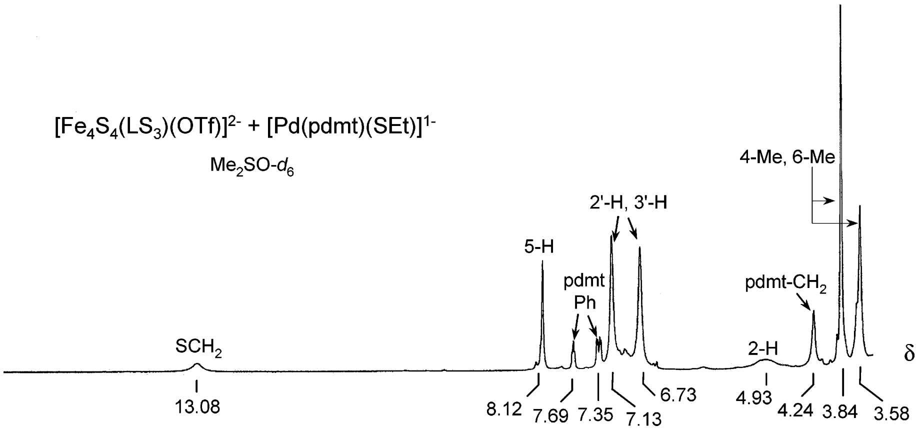

Figure 8. ^{1}H NMR spectrum of a solution initially containing equimolar cluster **14** and complex **2b** in Me$_2$SO solution. The reactants form **15** in a thiolate transfer reaction.

Scheme 5. Reactions Based on Triflate Cluster **14**: Formation of **15** by Thiolate Transfer from Ni^{II}/Pd^{II} Complexes in Acetonitrile or Me$_2$SO, Bridged Assembly **20** (Not Isolated) by Reaction with [Ni(pdmt)(SEt)]$^-$ in Dichloromethane, and Bridged Double Cubane **21** by Reaction of Et$_3$NH$^+$ and [Fe$_4$S$_4$(LS$_3$)(SEt)]$^{2-}$ in Acetonitrile and Crystallization by Addition of Ether

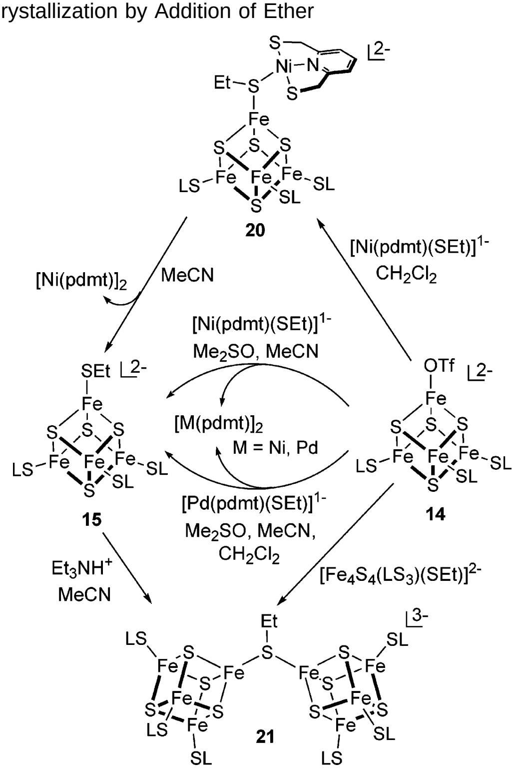

that, in the solvents utilized, reaction 5 proceeds by thiolate dissociation. Consequently, thiolate transfer requires the presence of a dinuclear intermediate or transition state of the form [Ni···S(Et)···Fe], encouraging a further search for a detectable bridged species.

The equimolar system **2a**/**14** in dichloromethane behaves differently, as may be seen by reference to Figure 9A,B. The product spectrum (9B) does not contain signals due to the putative thiolate transfer product **15** (9A). Further, the 5-H shift is consistent with a thiolate ligand at the unique site, and the SCH$_2$ signal (δ 13.35) does not correspond to any previously encountered cluster species. The latter signal is displaced from δ 1.70 in diamagnetic **2a**, indicating that it is paramagnetically shifted by binding to the cluster. Examination of the reaction mixture down to 243 K reveals decreased isotropic shifts (Table 1) and no additional signals attributable to a cluster species. At all temperatures the methylene shifts do not correspond to **15**. We attribute these observations to the occurrence of reaction 6, which generates bridged assembly **20** with an unsupported Ni−(μ_2-SEt)−Fe bridge (Scheme 5). Note that the SCH$_2$ shifts of

$$[\mathrm{Fe_4S_4(LS_3)(OTf)}]^{2-} + [\mathrm{Ni(pdmt)(SEt)}]^{-} \rightarrow [\{\mathrm{Ni(pdmt)(SEt)}\}\mathrm{Fe_4S_4(LS_3)}]^{2-} + \mathrm{TfO}^{-} \quad (6)$$

20 and **19** (δ 13.32 in CD$_3$CN, Figure 5D) are nearly the same. Cluster **19** contains the Ni−(μ_2-SCH$_2$R′)−Fe fragment proposed in **20** (but with a different R′ group). Also observed in Figure 9B are several pdmt signals which, because of signal overlap, cannot be specifically assigned. In dichloromethane, complex **2a** reacts with the solvent to form ca. 50% [Ni$_2$(pdmt)$_2$] (δ 3.66, 4.06) and unidentified species. The spectrum of this solution does not contain the resonance at δ 13.35. Reactions of terminally coordinated thiolates with chlorinated solvents have been observed previously.[26,54]

The signal at δ 13.35 is not shifted when the intial mole ratio **2a**:**14** is 2.3 or 8.9, indicating that the chemical shift is limiting. Under these conditions, a small amount of thiolate cluster **15** (<10% of total cluster product) is formed. As shown in Figure 9C, the system can be reversed in the form of reaction 7. Addition of acetonitrile to afford a 3:7 v/v acetonitrile/

$$[\{\mathrm{Ni(pdmt)(SEt)}\}\mathrm{Fe_4S_4(LS_3)}]^{2-} \rightarrow [\mathrm{Fe_4S_4(LS_3)(SEt)}]^{2-} + {}^{1}/_{2}[\mathrm{Ni_2(pdmt)_2}] \quad (7)$$

dichloromethane solution completely abolishes the signals assigned to **20**, which are replaced by those of **15** and [Ni$_2$(pdmt)$_2$]. Evidently, the Ni^{II} site is subject to attack by the donor solvent, causing rupture of the weakened Ni−SEt bridge bond. Complex **2a** itself is stable in acetonitrile. The cause of the lack of formation of a bridged Pd^{II} assembly is not clear but presumably lies in the greater stability of [Pd$_2$(pdmt)$_2$] vs [Ni$_2$(pdmt)$_2$].

Thiolate-Bridged Fe$_4$S$_4$ Double Cubane. During the course of substitution reactions of thiolate cluster **15**, we observed that reaction with Et$_3$NH$^+$ in acetonitrile followed by solvent removal and crystallization of the residue from acetonitrile/ether

---

(54) Segal, B. M.; Hoveyda, H. R.; Holm, R. H. *Inorg. Chem.* **1998**, *37*, 3440−3443.

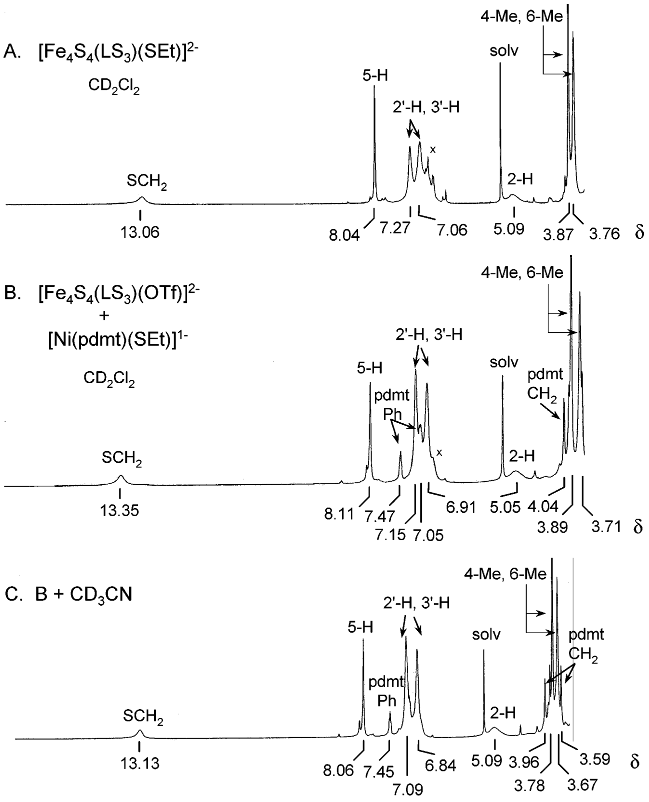

Figure 9. ^{1}H NMR spectra of cluster **15** (A), a solution initially containing equimolar **14** and complex **2a** (B), and solution B diluted with CD_3CN (C). Spectrum B is interpreted as bridged assembly **20**; spectrum C corresponds to **15**. The pdmt signals in spectrum B may arise from the bridged species and $[Ni_2(pdmt)_2]$; in spectrum C they are due to the dimer.

afforded the hitherto unknown double cubane **21**. The cluster is formed by the apparent stoichiometry of reaction 8. The

$$2[Fe_4S_4(LS_3)(SEt)]^{2-} + Et_3NH^+ \rightarrow [\{Fe_4S_4(LS_3)\}_2(SEt)]^{3-} + EtSH + Et_3N \quad (8)$$

solvated Bu_4N^+ salt crystallizes with two inequivalent but nearly structurally identical double cubane clusters in the asymmetric unit. These clusters present the first structurally proven examples of a single unsupported thiolate bridge involving an Fe_4S_4 cluster. The structure of one cluster is shown in Figure 10; metric data for both clusters are presented in Table 2. Because of the large quantity of data, most parameters are summarized in terms of ranges or mean values. Our present interest in this cluster is primarily structural.

Ligand conformations are *aaaaaa* (all substituents on the same side of the central benzene ring) in cluster 1 and *aaaaab* in cluster 2 (not shown). Individual cubanes within a cluster can be described in terms of sets of Fe−S bond lengths, as in prior structural analyses.[42] In both clusters, mean values of bond lengths sort into 4 short + 8 long in one cubane and 4 short + 4 intermediate + 4 long in the other. Structural distortions of $[Fe_4S_4]^{2+}$ cores are neither predictable nor easily rationalized in the more than 40 structures that have been determined,[42] as is the case here. Overall, bond angles and distances are unexceptional, leaving the bridge units as the principal structural feature of the clusters. Bridge Fe−S−Fe angles are near 120° and Fe−S distances are 2.31−2.32 Å, resulting in Fe−Fe separations of 4.00 and 4.07 Å. Bridge distances are 0.05−0.06 Å longer than mean values of terminal Fe−SR bond lengths, signifying weaker interactions. These bridge parameters serve as a guide to those in assembly **20**, which as yet has not been crystallized. In particular, a similar lengthening and weakening of the Ni−SEt bond (2.183(1) Å)[33] in **2a** may be anticipated in assembly **20**.

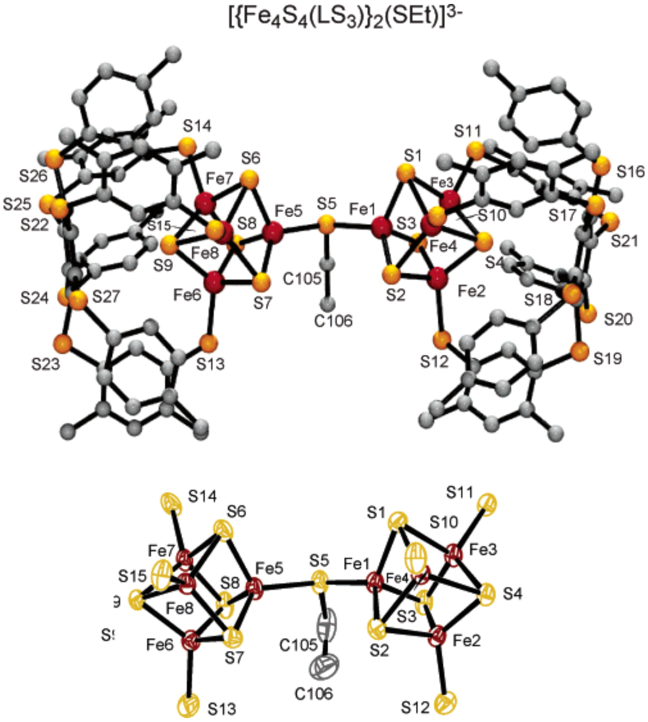

Figure 10. Structure of the entire cluster **21** (upper) and the bridged Fe_4S_4 portion (lower). The asymmetric unit contains two inequivalent clusters with very similar structures. One cluster is shown in a ball-and-stick presentation for clarity.

Summary. Our recent investigation of $Ni^{II}-(\mu_2\text{-}SR)-M^{II}$ bridging modes,[17] which emphasizes formation of the rhomb units $Ni^{II}(\mu_2\text{-}SR)_2M^{II}$, addresses steps (i) and (ii) in the construction of analogues of the A-cluster of CODH/ACS. This work presents the initial exploration of possible means of achieving step (iii), formation of an $[Fe_4S_4]^{2+}-(\mu_2\text{-}SR)-Ni^{II}$ bridge unit. As such, it is intended to complement and extend our earlier study. Within the manifold of 3:1 site-differentiated $Fe_4S_4(LS_3)$ species, the results reveal access to four clusters: **18**, with two mutually supportive $Fe-(\mu_2\text{-}SR)-Ni^{II}$ bridges; **19**, with one strong and one weaker bridge; **20**, with one unsupported bridge postulated from ^{1}H NMR spectra; and double cubane **21**, with one unsupported bridge. Previously prepared double cubanes are sulfide- or selenide-bridged,[23,55−57] as exemplified by $\{[Fe_4S_4(LS_3)]_2S\}^{4-}$. The higher negative charge and basicity of the bridge atoms are more conducive to bridge formation than those of thiolate. The stability of cluster **18** is indicated by its formation via an unexpected cleavage reaction of binuclear complexes (**6**−**10**), several with M^{II} components introduced to

---

(55) Stack, T. D. P.; Carney, M. J.; Holm, R. H. *J. Am. Chem. Soc.* **1989**, *111*, 1670−1676.
(56) Challen, P. R.; Koo, S. M.; Dunham, W. R.; Coucouvanis, D. *J. Am. Chem. Soc.* **1990**, *112*, 2455−2456.
(57) Huang, J.; Mukerjee, S.; Segal, B. M.; Akashi, H.; Zhou, J.; Holm, R. H. *J. Am. Chem. Soc.* **1997**, *119*, 8662−8674.
(58) Nicolet, Y.; Lemon, B. J.; Fontecilla-Camps, J. C.; Peters, J. W. *Trends Biochem. Sci.* **2000**, *25*, 138−143.
(59) Peters, J. W.; Lanzilotta, W. N.; Lemon, B. J.; Seefeldt, L. C. *Science* **1998**, *282*, 1853−1858.

retard M^{II}−SR bond cleavage. None of these clusters contain a binuclear fragment with Ni^{II} atoms as simulators of distal and proximal sites.

Overall, this work and other reports that precede it[25,26] make it evident that two intramolecular bridges of the desired type are attainable using a cis-planar Ni^{II}−S_2N_2 complex, and that a single unsupported bridge is achievable but less robust. Protein folding may contribute to the stabilization of the $[Fe_4S_4]^{2+}$−(μ_2-S_{Cys})−Ni^{II} interaction in CODH/ACS. Further approaches to the A-cluster may require a covalent link between the Fe_4S_4 and nickel-containing units in order to provide a juxtaposition of these two units favorable to bridge formation and stability. Finally, the bridge type realized in **21** is relevant to the Fe−(μ_2-SR)−Fe interaction that connects an Fe_4S_4 cluster to the dinuclear H-cluster in iron hydrogenases.[58,59]

Acknowledgment. This research was supported by NIH Grant GM 28856. We thank Drs. C. Chiou and R. Panda for experimental assistance and Dr. Chiou for the initial preparation of cluster **19**.

Supporting Information Available: Tables of crystallographic data for mononuclear and binuclear complexes and clusters (S1), bond distances and angles of complexes **4**−**7** (S2), and bond distances and angles of $[\{Ni(L_O\text{-}S_2N_2)\}M(SCH_2CH_2PPh_2)]^+$ (S3) (PDF); X-ray crystallographic files for the 12 compounds in Table S1 (CIF). This material is available free of charge via the Internet at http://pubs.acs.org.

JA040222N